

# Finite Size Scalings and the Nuclear Liquid-Gas Phase Transition

Johan Helgesson<sup>1</sup>, Roberta Ghetti<sup>2</sup>,  
Luciano G. Moretto<sup>3</sup>, Dmitry E. Breus<sup>3</sup>, James B. Elliott<sup>3</sup>,  
Larry W. Phair<sup>3</sup>, and Gordon J. Wozniak<sup>3</sup>

<sup>1</sup>*School of Technology and Society, Malmö University, Sweden*

<sup>2</sup>*Department of Physics, Lund University, Sweden*

<sup>3</sup>*Nuclear Science Division, Lawrence Berkeley National Laboratory, Berkeley, USA*

## Abstract

Recent analyses of multifragmentation data in terms of Fisher's model have led to the estimate of the coexistence curve of finite nuclear matter as well as of the location of the critical point. In order to extrapolate those results to infinite nuclear matter, finite size effects have to be taken into account. Guided by the finite size behavior of the three-dimensional Ising model, we propose a modified Fisher Droplet model expression that incorporates surface and correlation length effects.

## 1 Introduction

One of the most intriguing questions of nuclear physics during the last decade is the identification of the various phase transitions theoretically predicted to happen in nuclear matter. Recently, by studying the cluster abundance as a function of mass and temperature in terms of Fisher's theory of clusterization in vapor, the quest for discovery of the liquid to vapor phase transition in nuclei has progressed to the complete description of the phase diagram from low temperatures up to the critical point [1, 2].

In Refs. [1, 2], estimates have been made of the pressure-temperature and temperature-density coexistence curve of finite nuclear matter as well as of the location of the critical point. Those estimates are obtained for a hot piece of nuclear matter produced in a nuclear collision, with no more than a few hundreds nucleons. Thus, in order to obtain the phase diagram for infinite nuclear matter, finite size scalings and Coulomb effects have to be introduced. Many theoretical works have investigated different methods to take such effects into account [3, 4, 5, 6, 7, 8]. However, it is unclear at the moment what the proper scaling laws should be. It is the purpose of this paper to demonstrate

such scalings in simple models, to discuss their origins in universal properties of thermal systems, and to shine some light on their applicability on nuclear finite systems.

Continuous phase transitions portray critical behavior and are ruled by universal properties and exhibit universal scalings. In particular, it is well known that the ferromagnetic phase transition, mimicked by the zero field Ising model, belongs to the same universality class as the liquid-gas phase transition, described by the Lattice-Gas model. In this paper we are going to utilize the Ising model to investigate finite size scalings and their implications for the nuclear liquid-gas phase transition.

## 2 The Ising Model and the Nuclear Liquid Gas Phase Transition

The 3D-Ising model is the simplest model containing a thermal phase transition of first order terminating at a critical point [9]. The Hamiltonian of the Ising model has two terms, the interaction between nearest neighbor (*n.n.*) spins in a fixed lattice and the interaction between the fixed spins and an external field  $H_{\text{ext}}$

$$H = -J \sum_{i,j=(n.n.)} s_i s_j - H_{\text{ext}} \sum_i s_i, \quad (1)$$

where  $J$  is the strength of the spin-spin interaction. Throughout this work the external field will be taken zero,  $H_{\text{ext}} \equiv 0$ . Connection with a liquid-gas system can be made by identifying the liquid phase with spin sites of majority spins and the gas phase with spin sites of minority spins. Clusters can be defined by grouping neighboring sites of equal spin. “Physical clusters” in the Ising model are identified using the Coniglio-Klein prescription[10], since it is known that “geometrical cluster” distributions do not show the same critical behavior as other physical quantities of the Ising model. In the absence of an external field, the liquid phase is in coexistence with the gas phase below the critical temperature, where a large “percolating” cluster (liquid phase) and distributions of smaller clusters of both majority (droplets of liquid) and minority (bubbles of gas) spin are found. Details about the numerical calculations of the Ising model can be found in Refs. [11, 12].

The Ising model captures the essential features observed in experiments on the nuclear liquid-gas phase transition [13]. In particular, the Ising model contains both reducibility and thermal scaling, that have been found to be quite pervasive in all multifragmentation reaction data [14]. Reducibility is the property of the  $n$ -fragment emission probability of being expressible in terms of an elementary one-fragment emission probability. This property can occur only when fragments are created independently from one another, and it coincides with stochasticity. The Ising fragment distributions exhibit thermal scaling, that is the linear dependence of the logarithm of the one-fragment probability with  $1/T$  (an Arrhenius plot). This signifies that the production probability

for a fragment of type  $i$  has a Boltzmann dependence  $p_i = p_0 \exp(B_i/T)$ , where  $B_i$  is a barrier corresponding to the emission process. This feature has been amply verified in nuclear multifragmentation [14, 17].

## 2.1 Description of the Vapor: the Fisher Droplet Model

The features of reducibility and thermal scaling discussed above can be found in the scaling proposed by Fisher [18, 19] to describe the concentration of droplets in a vapor, for macroscopic fluids. This is based on the simple idea that a real gas of interacting particles can be treated as an ideal gas of clusters of various sizes in chemical equilibrium. Fisher's formula for the concentration  $n(A, T)$  of clusters of size  $A$  in a vapor at temperature  $T$  is [18, 19]

$$n(A, T) = q_0 A^{-\tau} \exp(c_0 A^\sigma / T_c) \exp(\Delta\mu A / T) \exp(-c_0 A^\sigma / T) \quad (2)$$

where  $q_0$  is a normalization constant,  $\tau$  is a topological critical exponent,  $c_0$  is a zero temperature surface energy coefficient,  $\sigma$  is a surface to volume critical dimensionality exponent. Finally,  $\Delta\mu$  is the difference of the chemical potentials associated with the liquid and the gaseous phase, and it indicates the distance of the system from coexistence. Along the phase coexistence line,  $\Delta\mu=0$  and the cluster concentration reduces to

$$n(A, T) = q_0 A^{-\tau} \exp(-c_0 \epsilon A^\sigma / T), \quad (3)$$

where  $c_0 \epsilon A^\sigma$  is the surface free energy of a droplet of size  $A$  and the reduced temperature  $\epsilon = 1 - T/T_c$  ensures that the surface free energy goes to zero at the critical temperature  $T_c$ .

## 3 Finite Size Scalings

### 3.1 Phase Transitions in Finite Systems

A finite system with a surface has a lower binding energy than the corresponding infinite system. This means that clusters are easier produced in the finite system, which could imply that the location of the critical point is different as compared to the location in a corresponding infinite system. In addition, there are other finite size effects that may affect the critical behavior. As the system approaches the critical regime, fluctuations of all sizes appear, and changes in one point of the system may easily propagate and affect the entire system. One says that the correlation length increases, and for an infinite system, the correlation length goes to infinity as the critical temperature is approached. For a system of finite size, the range of the correlation length reaches the system size before the critical point, of an infinite system, is reached. This may cause the critical point to be shifted as compared to the infinite system.

The Ising model lends itself to study finite size scalings by determining how the critical quantities change as the size of the lattice is changed. Finite

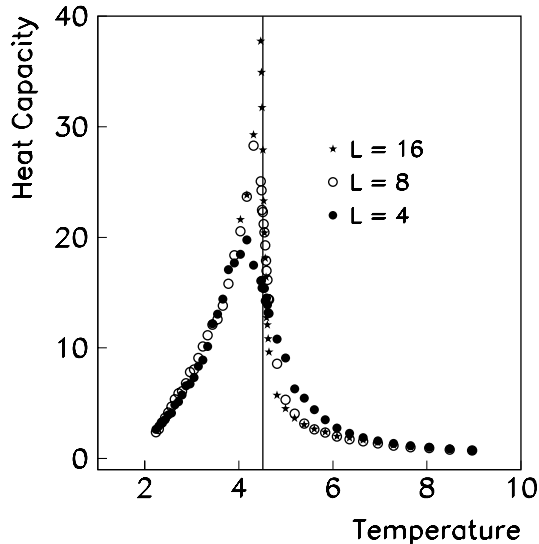


Figure 1: The heat capacity calculated in the 3D-Ising model for cubic lattices of different sizes ( $L_0 = 4, 8, 16$ ) and *obc*. The vertical line indicates  $T_c^\infty$ .

size scaling effects can be studied by varying the lattice size with both open boundary conditions (*obc*)<sup>1</sup> and with periodic boundary conditions (*pbc*). Even if lattices with *pbc* are expected to mimic true infinite systems, finite size effects are observed also with *pbc* [23], as it will be discussed later on. This kind of approach to the study of finite size scalings has been discussed long ago [23, 24, 25], and it was shown that different thermodynamic response functions scale in different ways, but all converge to the same value of the critical temperature in the thermodynamical limit [24, 25].

### 3.2 Finite Size Scalings from the Critical Behaviour of the Heat Capacity

Before turning to the cluster distributions, we discuss the scaling of the critical temperature from the change in the heat capacity [26], calculated for systems of different sizes with *obc*. The specific heat is determined from the fluctuations of the internal energy and its variation with temperature is studied. For an infinite system, the specific heat displays a sharp lambda-type singularity at the critical temperature  $T_c^\infty$  of a liquid-gas phase transition. The finite system specific heat, on the other hand, does not exhibit such a sharp singularity but has a large peak at a temperature  $T_c(L_0)$  which approaches  $T_c^\infty$  as the side  $L_0 \rightarrow \infty$ . This is seen in Fig. 1. The temperature  $T_c(L_0)$  can be regarded as the critical temperature for the finite system of size  $L_0^3$ , so that the effect of the

<sup>1</sup>With *obc* we take the interaction at the lattice surface to be  $+J$ , which is the same interaction that is taken at internal cluster surfaces with neighboring sites of opposite spin.

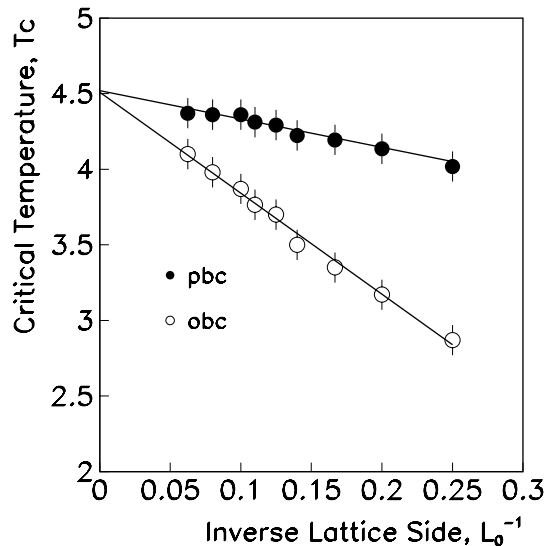


Figure 2: Finite size scaling of the critical temperature of the 3D-Ising model, for lattices of different sizes ( $L_0=4-10,12,16$ ). Dots: results for lattices with periodic boundary conditions. Circles: results for lattices with open boundary conditions. Lines: straight line fits.

finite size is to shift the critical temperature to a lower value, and to turn the associated critical singularities into rounded finite peaks. Fig. 2 illustrates the scaling of the critical temperature deduced from the position of the maximum of the heat capacity for lattices of various size with both *pbc* (dots) and *obc* (circles). The straight line fits are quite accurate and yield

$$T_c(L_0)/T_c^\infty = 1 - 0.4L_0^{-1} \quad (4)$$

for *pbc*, and

$$T_c(L_0)/T_c^\infty = 1 - 1.5L_0^{-1} \quad (5)$$

for lattices with *obc*, which more closely represent the case of finite systems like nuclei. The accepted value of the critical temperature for the 3D-Ising model is  $T_c = 4.513J/k_b$ , yielded by Monte Carlo calculations.

The linear scaling of the critical temperature suggested by these Ising calculations can be interpreted for nuclei in the following way. Nuclei are thin skinned systems, and they are well described as a fluid whose binding energy depends on the interplay of the bulk and the surface energies, plus higher order corrections (Coulomb and shell effects), as in the liquid-drop model. In the infinite Ising model there is only one parameter, the coupling constant  $J$ , that has the dimensions of energy. Therefore the critical temperature should scale as the “binding energy per site”. The binding energy is higher in the infinite system as compared to the finite system. In the finite system, clusters near the

surface are less bound and easier to produce and we expect that the critical temperature should scale with an “effective binding energy per site”. For a system of size  $A_0$  we can write

$$\frac{T_c(A_0)}{T_c^\infty} = \frac{a_b A_0 + a_s A_0^{2/3}}{a_b A_0}. \quad (6)$$

Remembering that for leptodermous systems  $a_b \approx -a_s$  we have

$$\frac{T_c(A_0)}{T_c^\infty} \approx 1 - \frac{1}{A_0^{1/3}}. \quad (7)$$

We refer to this effect as to the *binding energy effect*. Interpreting this for the Ising lattice with size  $A_0 = L_0^3$ , we obtain

$$T_c(A_0)/T_c^\infty \approx 1 - 1/L_0. \quad (8)$$

However, eventhough *pbc* has no surface, a linear scaling of the critical temperature is observed in Fig. 2. We attribute this effect to the correlation length becoming of the same size as the system, before the infinite critical point is reached. This effect will be referred to, in the sequel, as the *correlation length effect*. We assume that the correlation length effect is the same for *pbc* and *obc* and that the difference between *pbc* and *obc* is due to the binding energy effect. Thus the binding energy effect yields a linear dependence of the critical temperature on  $1/L_0$  with a slope close to unity, in accordance with the naive expectation Eq. (8).

### 3.3 Finite Size Scalings from Cluster Distributions

In Sec. 3.2 the finite size scaling of the critical temperature was deduced from the maximum in the heat capacity for finite lattices of various sizes. However, our aim with this work is to study finite size scalings from cluster distributions, and to discuss their implications for the nuclear data. We can get a simple estimate of finite size scalings by fitting the cluster distributions obtained for different lattice sizes with *pbc* and *obc* to Fisher’s formula, Eq. (3). In the fitting procedure, we allow the parameters  $T_c$ ,  $c_0$  and  $\sigma$  to vary linearly with the lattice side  $L_0$ . The quality of the fits is illustrated by the scaling presented in Fig. 3, where we plot the cluster yield distributions  $n(A, T)$  scaled by the factor  $q_0 A^{-\tau}$ , against the quantity  $c_0 \epsilon A^\sigma / T$ . For the periodic boundary conditions the collapse of the data points onto a single line indicates a good fit with Eq. (3). Also for open boundary conditions the fit is good, but with a somewhat larger spreading of the data points. The fits for *pbc* yield the parameter values

$$\begin{aligned} c_0 &\approx 12.3(1 + 2.36/L_0), \\ \sigma &\approx 0.740(1 - 1.23/L_0), \\ T_c &\approx 4.51(1 + 0.043/L_0), \end{aligned} \quad (9)$$

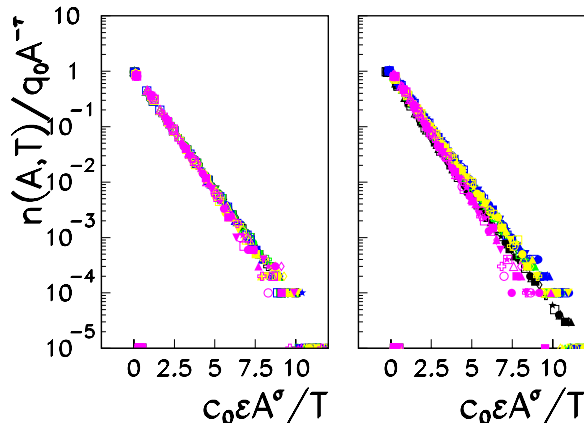


Figure 3: Collapse of the Fisher scaled cluster size distributions when Eq. (3) is used, for periodic (left panel) and open (right panel) boundary conditions. The colors represent different lattice sizes ( $L_0 = 8, 12, 16, 24, 32$ ). The symbols represent different cluster sizes ( $A = 11-20$ ).

while the parameters obtained for *obc* are

$$\begin{aligned}
 c_0 &\approx 12.8(1 - 0.85/L_0) , \\
 \sigma &\approx 0.611(1 + 2.00/L_0) , \\
 T_c &\approx 4.60(1 - 1.13/L_0) .
 \end{aligned}
 \tag{10}$$

For *obc* there is a strong dependence on the system size for all parameters, while the contributions from the correlation length effect, seen in the in the parameter variation for *pbc*, are smaller. Once again assuming that the correlation length effect is the same for *pbc* and *obc* and that the difference between *pbc* and *obc* is due to the binding energy effect, the binding energy effect yields a linear dependence of the critical temperature on  $1/L_0$  with a slope close to unity, in accordance with the naive expectation of Eq. (8).

To clarify the origin of these observations, we devote the next section to investigating Fisher's expression for cluster concentrations in some detail.

## 3.4 Reexamining Fisher's Expression for Cluster Concentrations

### 3.4.1 Cluster Surface Concentrations

The cluster concentration  $n(A, T)$  in Eq. (3) is an approximation to the more complete description  $n(S, A, T)$  which is the concentration of clusters of size  $A$  with surface  $S$  at the temperature  $T$ . The concentration may be written

[19] as a product of a combinatorial factor  $g(S, A)$  and a Boltzmann factor,  $\exp(-E_S/T)$

$$n(S, A, T) = g(S, A) \exp(-E_S/T) . \quad (11)$$

The first factor,  $g(S, A)$  depends only on the intrinsic properties of the cluster. It represents the number of different ways  $A$  sites can be combined to give the surface  $S$ . The surface part of the cluster energy is taken as  $E_S = cS$  with  $c$  being the surface tension and  $S$  denoting the total surface area (including also the area of eventual holes). The original Fisher expression, Eq. (3), is obtained by replacing  $S$  in Eq. (11), with the average surface  $\bar{S} = a_0 A^\sigma$ , assuming the combinatorial factor to be of the form [19]

$$g(\bar{S}, A) = \text{const } \bar{S}^{-\tau/\sigma} \exp[\varpi \bar{S}], \quad (12)$$

where  $\varpi$  is an entropy density. For cluster distributions, the critical temperature is identified with the temperature at which the distributions show a power law dependence on the cluster size. Physically, this appears when the surface free energy vanishes. From the surface free energy vanishing at  $T = T_c$ , it follows that

$$0 = \varpi \bar{S} - \frac{c\bar{S}}{T_c^\infty} \quad (13)$$

From this condition we can express  $\varpi$  in terms of  $c$  and  $T_c$ , and by also using  $c_0 = c a_0$ , Fisher's original expression Eq. (3) is recovered.

For small clusters it is possible to calculate the combinatorial factor,  $g(S, A)$  exactly, and thus it is possible to make direct comparisons between the predictions of Eq. (11) and calculated cluster surface distributions. In two dimensions it is possible to calculate  $g(S, A)$  for all surfaces up to about  $A = 32$  [27]. It is found that a combinatorial factor and a Boltzmann factor only, is not sufficient to describe the cluster concentrations of geometrical clusters for temperatures in the vicinity of the critical temperature [28, 29]. When the system approaches criticality, correlation length effects lead to effective cluster-cluster interactions. These cluster-cluster interactions depend on the size of the lattice and show up as finite size scalings in the Fisher parameters when Eq. (3) is used to characterize the cluster concentrations, as seen for  $pb$  in section 3.3.

The effective finite size scalings originating from correlation length effects and appearing in the parameters  $c_0$ ,  $\sigma$  and  $T_c$ , are approximately taken into account, in the sequel of this work, by assuming a linear dependence on the lattice side

$$c_0 = c_0(A_0) = c_0^\infty (1 - b_c/L_0) \quad (14)$$

$$\sigma = \sigma(A_0) = \sigma_\infty (1 - b_\sigma/L_0) \quad (15)$$

$$\epsilon = 1 - T/T_c(A_0), \quad \text{with } T_c(A_0) = T_c^\infty (1 - b_T/L_0) . \quad (16)$$

### 3.4.2 Binding Energy Effect on the Cluster Surface Energy

We now turn to a *finite system with a surface*, like the nucleus or the Ising lattice with open boundary conditions (*obc*). As before, the correlation length effects lead to finite size scalings of the parameters  $c_0$ ,  $\sigma$  and  $T_c$ , when Fisher's original expression, Eq. (3), is used to describe cluster size distributions. In addition, the surface of the system causes a change of the binding energy of the system, which leads to appreciable finite size effects.

When the system has a surface, the cluster surface energy,  $E_S$ , needed to make a cluster with surface  $S$ , will be different from  $c^\infty S$ . One way to see this, is to note that clusters that are formed at the surface of the system do not create that part of their surface that coincides with the surface of the system. The reduction of the needed surface energy depends on both the cluster and the system size. We incorporate the average effect by writing  $E_S(A, A_0) = f_{E_S}(A, A_0)c^\infty \bar{S}$ .

When the emitting system is a droplet, the effective surface energy reduction can be estimated by considering that not only the cluster changes its surface energy, but also the emitting system (since it reduces its size from  $A_0$  to the size  $(A_0 - A)$ ). The total surface energy needed to emit a cluster of size  $A$  from a system of size  $A_0$ , is the surface energy of the cluster minus the gain of surface energy of the shrinking system

$$\begin{aligned} E_S(A) &- [E_S(A_0) - E_S(A_0 - A)] = c_0 A^\sigma - c_0 A_0^\sigma + c_0 [(A_0 - A)^\sigma] \\ &= c_0 A^\sigma f_{E_S}^{\text{Droplet}}(A, A_0) \end{aligned} \quad (17)$$

with

$$f_{E_S}^{\text{Droplet}}(A, A_0) = 1 + \left(\frac{A_0}{A}\right)^\sigma \left[ \left(1 - \frac{A}{A_0}\right)^\sigma - 1 \right]. \quad (18)$$

For other situations, like the formation of clusters in the Ising lattice, the system is constrained by the lattice structure and cannot relax to an arbitrary shape. In an Ising lattice with open boundary conditions, the clusters are formed predominantly in a region outside a large percolating cluster. Assuming that the percolating cluster occupies a region  $(1 - \nu_E)L_0^3$  of the lattice and that the energy needed to make clusters is supplied only in the remaining region  $\nu_E L_0^3$ , one can show that

$$f_{E_S}^{\text{Ising}}(A, A_0) \approx 1 - \frac{A^{1-\sigma}}{\nu_E L_0}, \quad (19)$$

where we also take into account that the lattice has a surface. The parameter  $\nu_E$ , representing the fraction of the lattice not occupied by the percolating cluster, may depend on temperature and lattice size. In the next section we demonstrate that this dependence can be taken into account in a simple form.

When a cluster is produced in a droplet that after the emission may readjust its configuration, also the combinatorial factor may effectively be modified in the same way as for the surface energy, previously described. We can express the probability as the product of the probabilities to form clusters, of size  $A$

and  $(A_0 - A)$  respectively, in an infinite system, divided by the probability to form a cluster of size  $A_0$ . Thus we make a replacement of the combinatorial factor  $g(\bar{S}(A))$ , where  $\bar{S}(A) = a_0 A^\sigma$ , by

$$\begin{aligned} g(\bar{S}(A)) \rightarrow g_{\text{total}} &= \frac{g(\bar{S}(A))g(\bar{S}(A_0 - A))}{g(\bar{S}(A_0))} \\ &= \text{const } A^{-\tau} \left(1 - \frac{A}{A_0}\right)^{-\tau} \exp [c_0^\infty A^\sigma f_{\text{gS}}(A, A_0)/T_c^\infty] \end{aligned} \quad (20)$$

When the emitting system is a droplet, it is straight forward to show that  $f_{\text{gS}}^{\text{Droplet}} = f_{\text{Es}}^{\text{Droplet}}$ , but for other situations where not all configurations are accessible, like the Ising lattice,  $f_{\text{gS}}$  in general may be different from  $f_{\text{Es}}$ . As for the correction of the cluster surface energy in the Ising lattice, a reasonable form may be obtained by assuming that only a fraction  $\nu_g$  of the lattice contributes to the readjustment of the combinatorial factor. Thus we take

$$f_{\text{gS}}^{\text{Ising}}(A, A_0) = f_{\text{gS}}^{\text{Droplet}}(A, \nu_g A_0) \quad (21)$$

### 3.5 Finite Size Scalings from Cluster Distributions - Re-examined

In this section we investigate Ising cluster concentrations, using the findings of Sec. 3.4. As pointed out in the previous section, the finite size effects may originate from either binding energy effects or from correlation length effects. We assume that the correlation length effects are the same for periodic and open boundary conditions, and the remaining finite size effects are due to the binding energy effect. The corresponding corrections of the cluster surface energy and of the combinatorial factor are extracted.

The Ising cluster distributions obtained with open boundary conditions are compared with the predictions of Eq. (3) with  $E_S = f_{\text{Es}} c_0 A^\sigma$ , and different forms of  $f_{\text{gS}}$ . The correlation length effects are taken into account by taking the parameters as in Eq. (9).

If either of, or both  $f_{\text{Es}}^{\text{Droplet}}$  and  $f_{\text{gS}}^{\text{Droplet}}$  are used for  $f_{\text{Es}}$  or  $f_{\text{gS}}$  respectively, no acceptable collapse is obtained. This suggests that the geometry of the Ising lattice puts constraints on the relaxation of the remnant (i.e. the remaining system  $A_0 - A$ ) as compared to a droplet.

In Fig. 4 we present the results obtained with  $f_{\text{Es}} = f_{\text{Es}}^{\text{Ising}}$  and

$$T_c [f_{\text{Es}}/f_{\text{gS}}] = 4.51(1 - 1.13/L_0). \quad (22)$$

The fit was obtained with  $\nu_E = 0.088 + 3.21/L_0$ . As illustrated in the figure, the collapse is very good, with only small deviations from a perfect fit for the smallest lattice  $L_0 = 8$ . Thus, taking into account the geometry of the Ising lattice and the "inactive" percolating cluster, a good scaling is obtained.

Emirically we find that taking  $f_{\text{gS}}^{\text{Ising}}(A, A_0) = f_{\text{gS}}^{\text{Droplet}}(A, \nu_g A_0)$  and  $\nu_g \approx 1.5\nu_E^3$ , Eq. (22) is reproduced to an accuracy of a few percent. This indicates

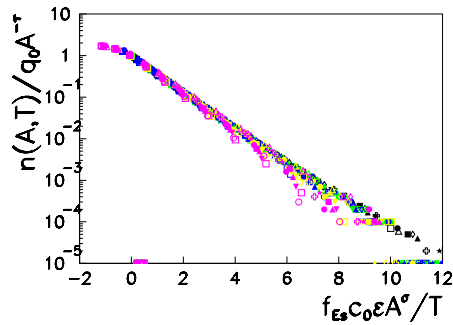


Figure 4: Collapse of the Fisher scaled cluster size distributions when  $f_{\text{Es}}^{\text{Ising}}$  is introduced for open boundary conditions. The colors represent different lattice sizes ( $L_0 = 8, 12, 16, 24, 32$ ). The symbols represent different cluster sizes ( $A = 11-20$ ).

that indeed only a fraction of the Ising lattice contributes to the readjustment of the combinatorial of the remnant, as was the case for the corrections of the surface energy.

## 4 Summary

The liquid-gas phase transition in nuclear matter has been the subject of numerous investigations in nuclear physics. Experimentally, the phase transition is looked for in heavy ion collisions, that produce a hot piece of nuclear matter with no more than a few hundred nucleons. Thus, finite size effects cannot be neglected when comparing experimental data with theoretical calculations for infinite nuclear matter. Lattice models can be used as a guideline to investigate the finite size effects. In particular, the liquid-gas phase transition belongs to the the same universality class of the Ising model, thus scaling functions generated with the critical Ising model constitute a hallmark for the liquid-gas phase transition universality class.

Traditionally, finite size scalings have been derived from the behavior of thermodynamical response functions, such as order parameter, magnetization, heat capacity, etc. Such thermodynamical quantities are not readily available from nuclear experiments. The novel approach presented in this paper is to derive scaling laws from the analysis of cluster distributions.

Both experimental and Ising cluster distributions are well described by the Fisher Droplet model. Within Fisher's formalism, the study of finite size scalings reduces to assessing the scaling laws of Fisher's critical parameters: the critical temperature,  $T_c$ , the surface energy coefficient,  $c_0$  and the surface to volume dimensionality exponent,  $\sigma$ . The scalings laws of the Fisher's param-

ters are understood in terms of two finite size effects: the *binding energy effect* and the *correlation length effect*. Both effects give important contributions and are needed to obtain the correct scaling of Fisher's parameters. The binding energy correction can be included by a simple expression based on either the properties of an emitting droplet or on properties of the Ising cluster, depending on the system at hand. Our findings indicate that it is important to include the binding energy effect both as corrections of energies and as corrections of combinatorial factors.

In the nuclear case, it is mainly the short range strong force that gives rise to bulk and surface energies, and thus a similar type of finite size scalings, as those discussed for the Ising model, are expected. Both binding energy and correlation length effects are important and present also in the nuclear case. When specialized to the nuclear case, the binding energy effect originates not only from the surface energy and from the combinatorial part (as in the Ising model) but also from all other energy terms and higher order corrections that may be relevant to describe the nuclear system. Specialized to the nuclear case, the combinatorial part can be identified with the level density, which energy averaged contains a size dependence. In addition, the nuclear system contains also the long range Coulomb force. The finite size effects on the Coulomb interaction [3, 5, 6, 30] can be incorporated by a similar approach as for the surface energy.

## References

- [1] J.B. Elliott *et al.*, Phys. Rev. Lett. **88**, 042701 (2002).
- [2] J.B. Elliott *et al.*, nucl-ex/0205004 (2002).
- [3] H.R. Jaqaman, A.Z. Mekjian and L. Zamick, Phys. Rev. C **29**, 2067 (1984).
- [4] H. Müller and B.D. Serot, Phys. Rev. C **52**, 2072 (1995).
- [5] J.N. De, B.K. Agrawal and S.K. Samaddar, Phys. Rev. C **59**, R1 (1999).
- [6] S.J. Lee and A.Z. Mekjian, Phys. Rev. C **63**, 044605-1 (2001).
- [7] A.H. Raduta and A.R. Raduta, Phys. Rev. Lett. **87**, 202701 (2001).
- [8] P. Pawłowski, Phys. Rev. C **65**, 044615 (2002).
- [9] K.G. Wilson, Rev. of Modern Phys. **47**, 773 (1975).
- [10] A. Coniglio and W. Klein, J. Phys. A **13**, 2775 (1980).
- [11] R.H. Swendsen and J-S. Wang, Phys. Rev. Lett. **58** 86 (1987).
- [12] L.-J. Chen, C.-K. Hu and K.-S. Mak, Comput. Phys. Commun. **66**, 377 (1991).

- [13] C.M. Mader *et al.*, LBNL-47575, nucl-th/0103030 (2001).
- [14] L.G. Moretto *et al.*, Phys. Rep. **287**, 249 (1997).
- [15] L. Beaulieu *et al.*, Phys. Rev. Lett. **81**, 770 (1998).
- [16] L.G. Moretto *et al.*, Phys. Rev. C **60**, 031601 (1999).
- [17] J.B. Elliott *et al.*, Phys. Rev. Lett. **85**, 1194 (2000).
- [18] M.E. Fisher, Physics **3**, 255 (1967).
- [19] M.E. Fisher, Rep. Prog. Phys. **30**, 615 (1969).
- [20] C.S. Kiang and D. Stauffer, Z. Physik **235**, 130 (1970).
- [21] D. Stauffer and C.S. Kiang, Advances in Colloid and Interface Science, **7**, 103 (1977).
- [22] L.G. Moretto *et al.*, nucl-ex/0209009 (2002).
- [23] M.E. Fisher and A.E. Ferdinand, Phys. Rev. Lett. **19**, 169 (1967).
- [24] D.P. Landau, Phys. Rev. **B 13**, 2997 (1976).
- [25] A.M. Ferrenberg and D.P. Landau, Phys. Rev. B **44**, 5081 (1991).
- [26] K. Binder, Physica **62**, 508 (1972).
- [27] Iwan Jensen, private communication (2002).
- [28] B. Borštnik and D. Lukman, Phys. Rev. E **60**, 2595 (1999).
- [29] D. Breus *et al.*, (in preparation).
- [30] B.K. Srivastava *et al.* Phys. Rev. C **64**, 041605R (2001).